Microelectronic Engineering 86 (2009) 2241–2246

Contents lists available at ScienceDirect

Microelectronic Engineering

journal homepage: www.elsevier.com/locate/mee

Pore sealing of mesoporous silica low-*k* dielectrics by oxygen and argon plasma treatments

Chih-Chieh Chang, Fu-Ming Pan *, Ching-Wen Chen

Department of Materials Science and Engineering, National Chiao-Tung University, 1001, Ta Hsueh Rd., Hsinchu 30050, Taiwan, ROC

ARTICLE INFO

Article history:
Received 7 November 2008
Received in revised form 3 February 2009
Accepted 20 March 2009
Available online 30 March 2009

Keywords:
Plasma treatment
Pore sealing
Low-*k* dielectric

ABSTRACT

In this study, we have prepared surfactant templated mesoporous silica thin films as the ultralow-*k* dielectrics and a TaN_X thin film deposited by plasma enhanced atomic layer chemical vapor deposition (PE-ALCVD) using $TaCl_5$ as the gas precursor was used as the diffusion barrier. Without any surface modification for the dielectric layer, Ta atoms could easily diffuse into the mesoporous layer seriously degrading dielectric properties. O_2 and Ar plasmas have been used to modify the surface of the mesoporous dielectric in a high density plasma chemical vapor deposition (HDP-CVD) system, and both of the treatments produced a densified oxide layer a few nanometer thick. According to transmission electron microscopy and Auger electron spectroscopy, the pore sealing treatment could effectively prevent Ta atoms from diffusing into the mesoporous dielectric during the PE-ALCVD process.

1. Introduction

Future generations of integrated circuits require continual introduction of low-dielectric constant (low-*k*) dielectrics with decreasing *k* value to reduce resistance–capacitance (RC) delay, power and heat dissipation, and interline cross-talk. A wide range of approaches have been developed to lower the *k* value of dielectrics, e.g., incorporation of carbon and hydrogen into silica network by chemical vapor deposition (CVD) [1,2], micropore or mesopore formation in dielectrics by spin-coating of silica sol, and by porogen removal [3–5]. Among various low-*k* dielectrics, porous silica materials are generally believed to be one of the most promising candidates for interlayer dielectrics at technology nodes of 60 nm and below because they are chemically compatible with contemporary IC processes and a $k < 2.0$ can be easily obtained owing to a high porosity. However, before being implemented in Cu damascene processes, porous dielectrics need to overcome many integration challenges. One of the major concerns about integration of porous dielectrics into Cu interconnect technology is that surface pores are penetration pathway of adverse impurities into the porous dielectrics, such as moisture uptake during cleaning and plasma species diffusion during etching. Therefore, surface modification is imperative for porous low-*k* dielectrics being integrated into Cu damascene process. This is particularly true when the diffusion barrier layer is deposited by atomic layer CVD (ALCVD).

Because of the self-limiting surface reaction kinetics, ALCVD is very suitable for deposition of ultrathin barrier layers with an accurately controlled thickness as well as an excellent conformity and uniformity. However, gas precursors can easily diffuse into porous dielectrics during ALCVD processes, degrading electrical properties of the low-*k* dielectrics. Many solutions have been attempted to alleviate the precursor penetration, such as capping layer deposition [6–8], plasma treatment [9–11], and etch-byproduct deposition [12,13]. In this work, we used O_2 and Ar plasma to modify the surface of surfactant templated mesoporous silica dielectrics by reconstructing the pore structure and thereby forming a densified surface layer to achieve the pore sealing. For most previous studies using plasma treatments, porous low-*k* dielectrics, such as MSQ and organic polymers, were generally hydrophobic in nature. The as-calcined mesoporous silica prepared in the study is intrinsically hydrophilic, and methylsilylation can be performed to improve hydrophobicity of the low-*k* dielectric [5]. In this work, the as-calcined mesoporous silica was directly subjected to the plasma treatment without any hydrophobicity pretreatment so that retardation of moisture uptake due to the pore sealing treatment could be investigated. To study the effectiveness of the pore sealing process on suppressing impurity diffusion, we deposited the TaN barrier layer on the as-calcined and plasma-treated mesoporous silica dielectric films by plasma enhanced-ALCVD (PE-ALCVD).

2. Experimental

The preparation method of the mesoporous silica thin film has been described previously [5]. In brief, a silica precursor sol was prepared by mixing and refluxing a solution of tetraethyl orthosilicate, H_2O, HCl, ethanol and a nonionic surfactant, Pluronic P-123.

* Corresponding author. Tel.: +886 3 5131322; fax: +886 3 5724727.
E-mail address: fmpan@faculty.nctu.edu.tw (F.-M. Pan).

0167-9317/$ - see front matter © 2009 Elsevier B.V. All rights reserved.
doi:10.1016/j.mee.2009.03.127

The precursor was spin-coated on precleaned 6 in *p*-type Si(100) wafers, followed by baking at 80–110 °C for 1 h to remove the aqueous solvent. The organic template molecules were removed from the mesoporous silica film by calcinations at 400 °C for 30 min in a furnace with air flow. Pore sealing of the as-calcined mesoporous silica by O_2 and Ar plasma treatments were performed in a high-density-plasma CVD system. The plasma treatments were carried out under the following process conditions: sample bias: 150 W; plasma power: 750 W; flow rate: 70 sccm; treatment time: 10 sec.

The PE-ALCVD system had a base pressure of 5×10^{-4} torr. During the PE-ALCVD TaN deposition, the stainless steel tube containing the solid $TaCl_5$ precursor was maintained at 110 °C to develop an adequate amount of $TaCl_5$ vapor and all the delivery lines were heated at 115 °C to prevent the precursor from condensation. Ar was used as the carrier gas. The thickness of the TaN barrier layer was controlled by optimizing the number of ALCVD process cycles. One ALCVD cycle consisted of a series of process steps, including introduction of $TaCl_5$, Ar purge, H_2/N_2 plasma nitridation, and Ar purge. TaN deposition was carried out at the substrate temperature of 300 °C.

Partially nitrided Ta (Ta(N)) was also sputter deposited on the mesoporous silica layer for thermal stability study. The sputter deposition of Ta(N) was carried out in a sputtering system (ULVAC SBH-3308RDE) at a power of 500 W. The base pressure of the sputter chamber was $<5 \times 10^{-7}$ torr. During the Ta(N) deposition, a gas mixture of Ar and N_2 with the flow rate ratio Ar/N_2 = 20:1 was used for Ta nitridation. The Cu film 20 nm in thickness was then deposited on the Ta(N) layer at a power of 1500 W in the same sputtering chamber without breaking the vacuum.

Density variation of the mesoporous silica films due to the plasma treatment was studied by high resolution specular X-ray reflectivity (SXR) (Panalytical X'Pert PRO). The SXR measurement was performed using a modified high resolution X-ray diffractometer using the Cu Kα radiation (0.15406 nm). The sample position was slightly shifted by 0.1° from the symmetric $\theta/2\theta$ position to avoid strong specular reflection. The reflectivity data was used to extract the density, thickness and roughness of the thin film sample using the simulation software (Wingixa™) bundled with the SXR system, which uses Parrat formalism for reflectivity to model the X-ray intensity scattered from a multilayer thin film [14,15].

Moisture uptake of the mesoporous silica film was studied by thermal desorption spectroscopy (TDS, Hitachi Tokyo Electronics TDS-APIMS). Auger electron spectroscopy (VG Microlab 350) depth profiling was performed to analyze elemental composition distribution in samples. Transmission electron microscopy (TEM, Philips tacnai 20) was used to study the interfacial microstructure of samples. Quick estimations of porosity of the as-calcined silica thin film was performed by a refractive index analyzer (n&k analyzer 1280) [16]. Dielectric property of the mesoporous silica film was measured with an HP 4145B semiconductor parameter analyzer using the metal–insulator–semiconductor (MIS) capacitor measurement structure with evaporated Al thin films as the electrodes.

3. Results and discussion

The as-calcined mesoporous silica thin film prepared as described in the experimental was about 250 nm thick. A quick evaluation by refractivity spectroscopy showed that the as-calcined mesoporous film had a porosity of ~41% [16]. According to our previous study, the average pore size of the mesoporous thin film was probably smaller than 40 Å [5]. The *k* value of the as-calcined mesoporous film was ~2.1 according to the CV measurement. Without any hydrophobicity treatment for the silica film, the *k* value increased to >4.0 after one week storage in the cleanroom ambient due to moisture uptake. According to SXR and TEM studies, a densified surface layer was formed on the mesoporous silica thin film after the plasma treatments.

3.1. Specular X-ray reflectivity analysis

SXR has been widely used to study material properties of thin films, such as mass density, film thickness and surface roughness, which can be deduced from SXR experimental data by curve fitting using modeling software [17,18]. Fig. 1 shows SXR spectra of the as-calcined and the plasma-treated mesoporous silica thin films within the Q_z range between 0 and 0.1. Q_z is the magnitude of X-ray momentum transfer in the film thickness direction and is defined as $(4\pi/\lambda)\sin\theta$, where λ is the wavelength of the X-ray and θ the grazing incident angle. The SXR result indicated that the surface region of the mesoporous silica film was significantly modified by the plasma treatments. The reflectivity within the Q_z range between 0.024 and 0.033 was shown in the inset of Fig. 1 to better illustrate the curve feature around the critical angle (θ_c). The two reflectivity drops were due to X-ray reflections around the critical angles characteristic for the mesoporous dielectric and the silicon substrate. The first θ_c around $Q_z \sim 0.026$ Å^{-1} was due to the mesoporous dielectric and the second one around $Q_z \sim 0.032$ Å^{-1} was due to the Si substrate. According to the best fit of simulation to the experimental data, the mass density of the as-calcined mesoporous silica film was 1.40 g/cm^3, assuming that a thin native oxide layer ~2 nm thick was present at the interface between the mesoporous layer and the Si substrate. If one assumed that the density of the pore wall of the mesoporous layer was comparable to that of the conventional silicon dioxide, 2.25 g/cm^3, the corresponding porosity of the as-calcined mesoporous silica would be 37.8%. This value was close to the porosity estimated by the refractivity measurement (~41%). The SXR spectra of the plasma-treated mesoporous silica thin film demonstrated a periodical oscillation feature largely different from that of the as-calcined film, indicating that the thickness of the mesoporous film was changed after the plasma treatment [16]. For the O_2 plasma-treated mesoporous silica film, one more top surface layer with a thickness of ~19.2 nm was required to obtain the best fit, and the simulated θ_c revealed a mass density about 82.2% that of the conventional SiO_2. The rest of the plasma-treated film had a porosity similar to that of the as-calcined mesoporous film. Compared with the O_2 plasma-treated mesoporous silica film, the Ar plasma-treated film showed a larger θ_c, as shown in the inset of Fig. 1, revealing that the top surface layer had a larger mass density. The top surface layer of the Ar

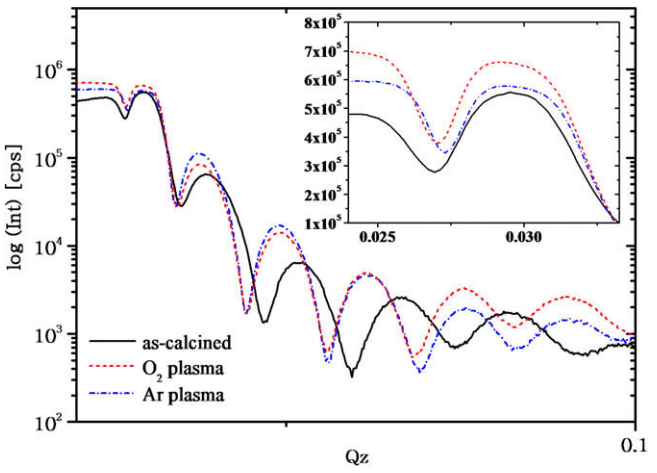

Fig. 1. SXR curves of the as-calcined and the plasma-treated mesoporous silica films.

plasma-treated mesoporous film had a fitted thickness of ~17 nm and the mass density was 87.3% that of the conventional SiO_2. The SXR analysis clearly indicated that the surface region of the mesoporous silica film was densified by the plasma treatments. The densified layer could seal opening pores on the surface of the mesoporous silica dielectric, thereby retard moisture uptake and impurity penetration during storage and subsequent processes.

3.2. Moisture uptake and leakage current

The as-calcined mesoporous silica thin film was inherently hydrophilic due to the presence of residual silanol terminal groups on the pore surface. Moisture uptake by these silanol groups can substantially degrade dielectric properties of the mesoporous silica thin film. In order to study the effect of the plasma treatments on moisture uptake of the mesoporous silica dielectric, the as-calcined and plasma-treated films were stored in the cleanroom ambient for 20 days. Fig. 2 shows thermal desorption spectra (TDS) of H_2O for the as-calcined and the plasma-treated mesoporous silica films. According to the TDS spectra of H_2O ($m/e = 18$), a large amount of water desorbed from the as-calcined mesoporous silica when the sample was thermally heated. Desorption of physisorbed water and weakly hydrogen-bonded water molecules prevailed around 100 and 250 °C, respectively [19,20]. On the other hand, water desorption from the plasma-treated mesoporous silica thin film was greatly reduced, suggesting that the plasma treatments could effectively impede moisture uptake. The retardation of water absorption could be ascribed to the presence of the plasma-densified surface layer formed on the mesoporous silica film.

Because of the densified surface layer, dielectric properties of the mesoporous silica dielectric can be significantly improved. The k value of the mesoporous silica was close to that of the as-calcined film (~2.1) right after the Ar and O_2 plasma treatments. But after one week storage in the cleanroom ambient, the k value could increase to 3.4, indicating that the densified surface layer still allow moisture uptake to take place because it had a mass density 12–18% less than the conventional oxide as revealed by the SXR analysis. The increase in k value with the storage time suggests that, after the plasma treatment, subsequent metallization processes should be proceeded as soon as possible, or hydrophobicity pretreatment, such as methylsilylation, should be performed before the plasma treatment. Fig. 3 shows the leakage current density

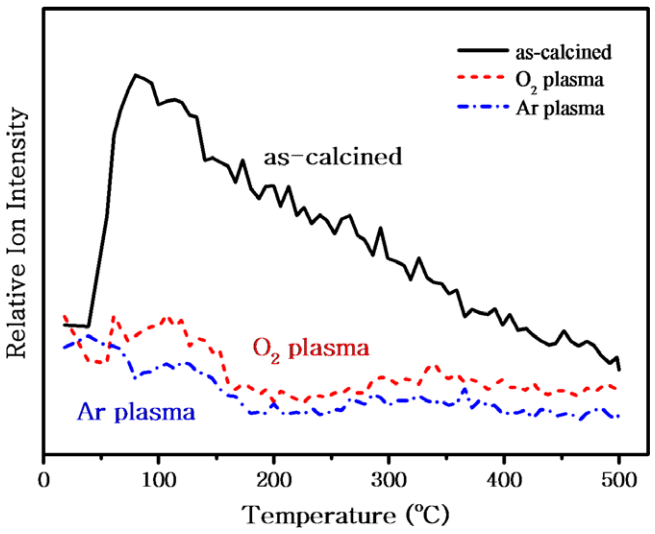

Fig. 2. TDS of H_2O ($m/e = 18$) for the as-calcined and the plasma-treated mesoporous silica films.

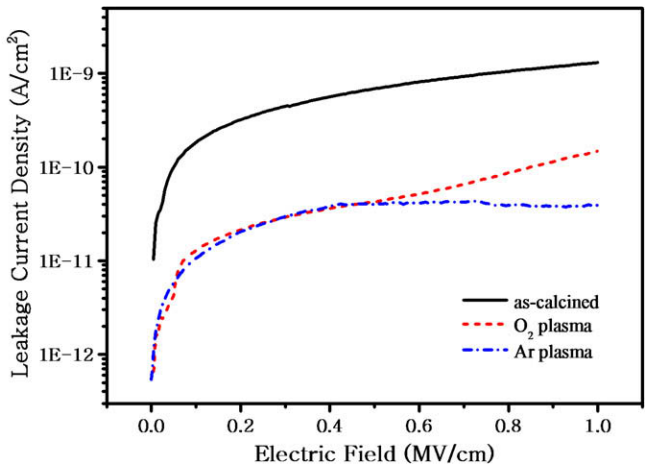

Fig. 3. Leakage current density versus electric field for the as-calcined and plasma-treated mesoporous silica films.

of the mesoporous silica film as a function of the electric field (J–E) before and after the plasma treatments. Prior to the plasma treatment, the mesoporous film showed a leakage current density of 1.3×10^{-9} A/cm^2 at a stress field of 1 MV/cm. The leakage current density dropped to 1.4×10^{-10} and 4.0×10^{-11} A/cm^2 after the O_2 plasma and Ar treatments, respectively. The one order of magnitude of decrease in the leakage current density after the plasma treatment can be attributed to the reduction of moisture uptake due to the plasma-densified surface oxide layer. During the J–E measurement, electrons injected into a thermal oxide thin film can be captured by water-related traps [21]. The porous nature of the mesoporous silica thin film could provide much more such traps in the film. After the plasma treatment, the leakage current of the mesoporous silica film was significantly reduced due to less adsorbed water molecules on the pore surface.

3.3. PE-ALCVD TaN barrier layer on the plasma-treated mesoporous SiO_2 dielectric

Without the densified surface layer, metallic impurities can easily diffuse into the mesoporous silica dielectric during the PE-ALCVD TaN deposition process. Fig. 4 shows TEM images of the PE-ALCVD TaN capped mesoporous silica dielectric with and without the plasma treatments. The TEM image of Fig. 4a clearly shows that Ta diffusion occurred when PE-ALCVD TaN was deposited on the as-calcined mesoporous silica at 300 °C. The dark band with a thickness of ~5 nm at the top of the sample was the PE-ALCVD TaN barrier layer. Below the barrier layer, a transition region with a gradual decrease in the mass contrast can be clearly observed. This was an indication that Ta had penetrated into the mesoporous silica layer during the TaN deposition. Auger depth profiles also provided the evidence of Ta diffusion in the mesoporous dielectric. The corresponding Auger depth profiles are shown in Fig. 5a. The Ta profile extended deeply into the mesoporous silica as compared with the nitrogen profile, indicating that Ta atoms had diffused into the mesoporous silica layer after the PE-ALCVD TaN deposition. It has been reported that the Ti precursor was found to penetrate into the porous low-k dielectric during the deposition of the TiN barrier layer on the porous low-k film by PE-ALCVD [22]. However, in this study, chlorine was not detected in the Auger depth profiling analysis (not shown in Fig. 5a), indicating that Ta penetration into the as-calcined mesoporous silica was due to inward diffusion of Ta atoms during the ALCVD process, but not due to diffusion of $TaCl_5$ precursor species.

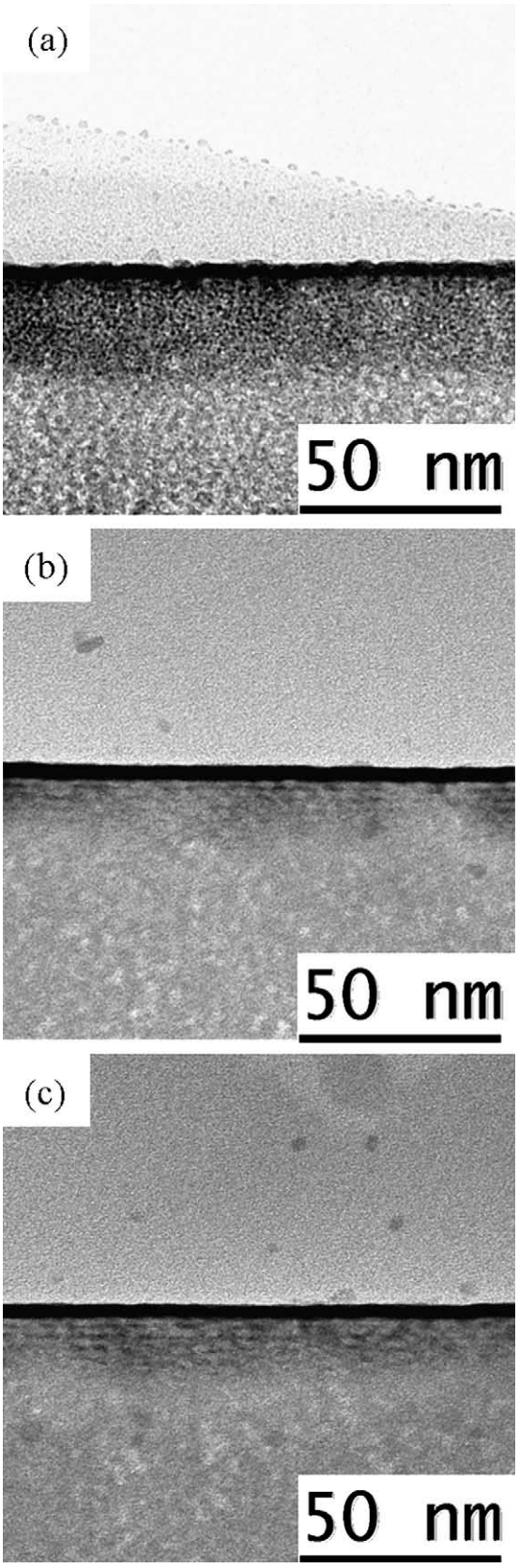

Fig. 4. Cross-sectional TEM images of the (a) as-calcined, (b) O_2 and (c) Ar plasma-treated mesoporous silica films.

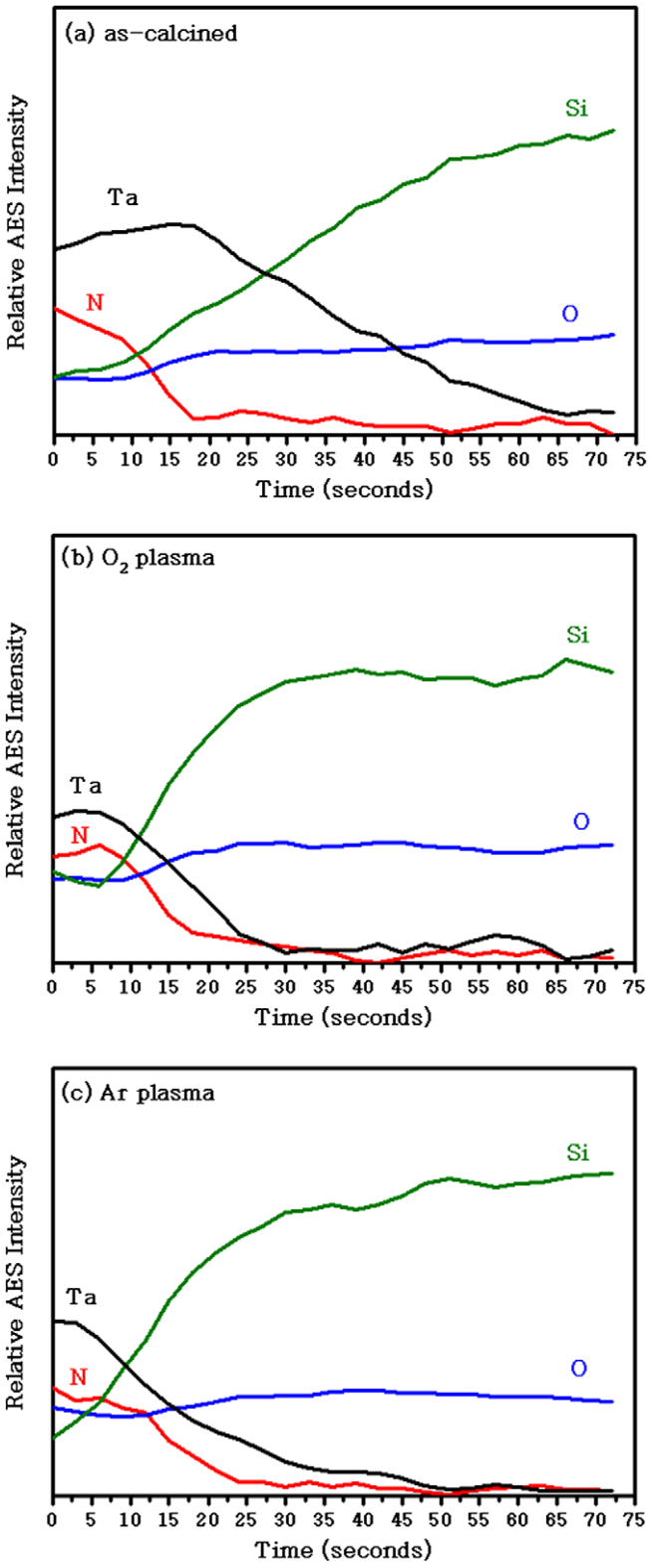

Fig. 5. AES depth profiles of the (a) as-calcined, (b) O_2 and (c) Ar plasma-treated mesoporous silica films.

When the mesoporous silica thin film was treated by O_2 or Ar plasma before the PE-ALCVD TaN deposition, Ta diffusion could be effectively prohibited by the plasma-densified oxide layer. Fig. 4b and c shows the TEM images of PE-ALCVD TaN capped mesoporous silica thin films treated with O_2 and Ar plasma, respectively. Below the TaN barrier layer of both the plasma-treated samples, there was a region with an image contrast slightly heavier

than that of the mesoporous silica layer. Fig. 5b and c are the corresponding Auger depth profiles of the two samples shown in Fig. 4b and c. For both the samples, the Ta and N profiles decayed in accordance with each other and did not extend far into the mesoporous silica layer as compared with that shown in Fig. 5a. Based on the Auger analysis, the plasma-treated mesoporous silica exhibited resistance against Ta diffusion during the PE-ALCVD TaN deposition. Therefore, observation of the interfacial region between the TaN and mesoporous silica layers shown in Fig. 4b and c is not due to Ta penetration, but likely the plasma-densified surface layer. The vague boundary between the interfacial region and the mesoporous silica layer shown in the TEM images was a consequence of plasma bombardment on the mesoporous silica layer, which could cause a statistically random distribution of substrate atoms as a function of the depth, during the plasma treatments. A rough estimation from the TEM images gives the interfacial region a thickness of ~20 nm, which is in agreement with the thickness of the densified surface layer derived from the SXR analysis discussed above. Combined with AES analyses, the TEM observations suggested that the plasma induced densified surface layer could effectively prevent Ta impurity from diffusing into the mesoporous silica dielectric during PE-ALCVD TaN deposition.

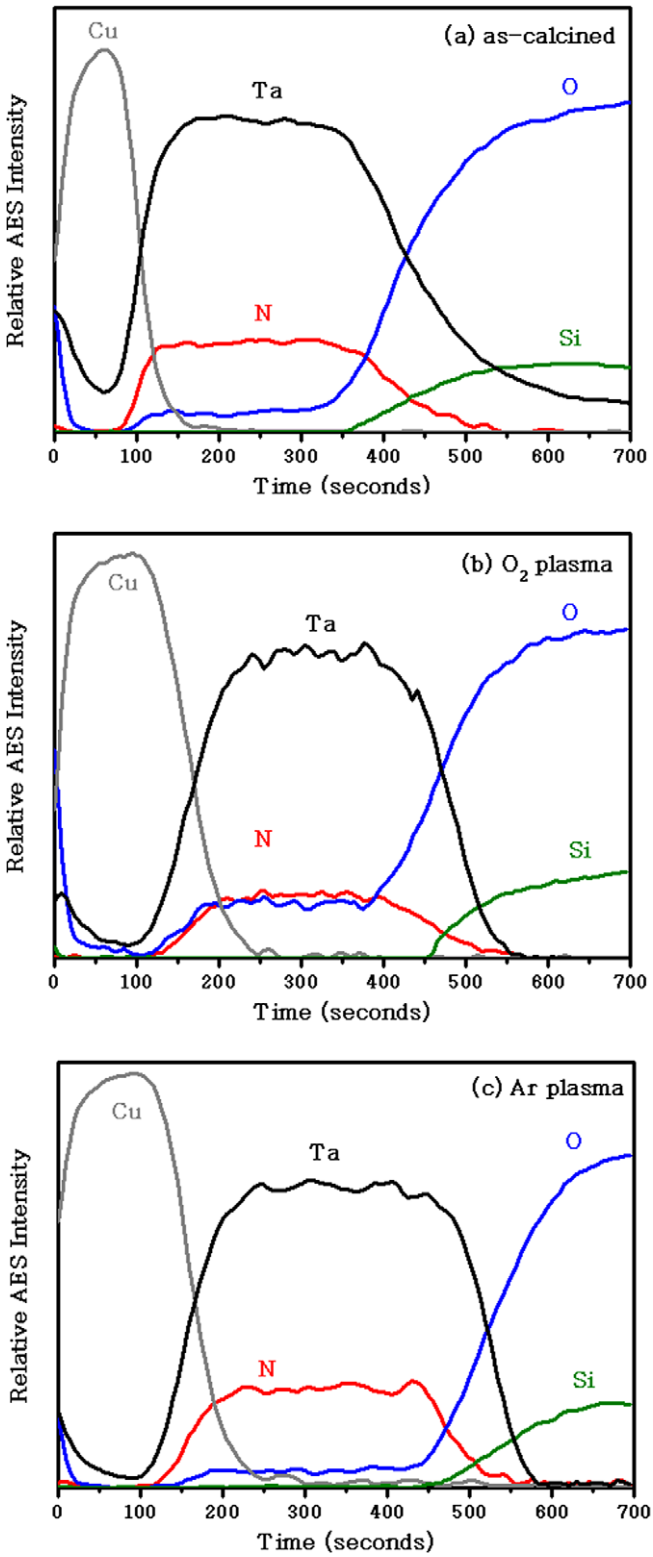

Fig. 6. AES depth profiles of the Ta(N)/Cu film stack was deposited on the (a) as-calcined, (b) O_2 and (c) Ar plasma-treated mesoporous silica films after annealing in vacuum at 600 °C for 30 min.

3.4. Thermal stability of the plasma-densified surface oxide

In order to study thermal stability of the plasma-densified oxide surface layer, a Ta(N)/Cu film stack was deposited on the mesoporous silica layer, and thermally annealed in vacuum at 600 °C for 30 min. Both the Cu and Ta(N) thin films were sputter-deposited, and had a thickness of 20 nm. Fig. 6 shows Auger depth profiles of the film stacks. Without the plasma treatment, serious diffusion of Ta atoms into the mesoporous silica thin film took place during the thermal anneal as shown by the extended tail of the Ta profile in Fig. 6a. Fig. 6b and c shows depth profiles of the film stacks with the mesoporous silica layer treated by the O_2 and Ar plasma, respectively. The quick Ta signal drop at the interface between the Ta(N) and the mesoporous silica films indicates that Ta diffusion into the mesoporous layer did not occur during the thermal anneal at 600 °C. The thermal stability study suggested that the plasma treatments are suitable for porous low-*k* dual-damascene processes in the aspect of the process temperature. It is worth noting that, compared with the film stacks with the as-calcined and the Ar plasma-treated mesoporous silica films, significant oxygen was present in the Ta(N) layer of the film stack with the O_2 plasma-treated mesoporous film. Because the anneal was carried out under a vacuum condition of $\sim 2 \times 10^{-3}$ torr, oxidation of the Ta(N) film due to inward diffusion of oxygen from the ambient was not likely. Moreover, the oxygen content was much less in the Ta(N) layer of the films stacks without the O_2 plasma treatment as shown in Fig. 6a and c. It was possible that residual oxygen species trapped in the mesoporous silica film during the O_2 plasma treatment diffused into the Ta(N) film during the high temperature anneal. It appears that, in respect of electrical conductivity, the O_2 plasma treatment may not be an appropriate pore sealing method for integration of the mesoporous silica film with the Ta(N) barrier layer.

4. Conclusions

Pore sealing of the mesoporous silica ultralow-*k* dielectric thin film was performed using O_2 and Ar plasma treatments. A densified layer <20 nm thick with a porosity of ~80–90% was produced under the plasma treatment conditions. The plasma-densified surface oxide layer could greatly reduce moisture uptake and thereby improve dielectric properties of the mesoporous dielectric. According to TEM and AES analyses, the densified surface layer could prevent Ta precursor species from penetrating into the mesoporous dielectric during PE-ALCVD deposition of the TaN barrier layer. Thermal stability study showed that the plasma treatments were effective to block impurity diffusion into the mesoporous low-*k* dielectric at temperatures as high as 600 °C.

Acknowledgements

This work was supported by the National Science Council of ROC under Contract No. NSC96-2221-E-009109-MY3. Technical supports from Prof. Y.M. Lee of National Tsing Hua University and from National Nano Device Laboratories are gratefully acknowledged.

References

[1] A. Grill, V. Patel, K.P. Rodbell, E. Huang, M.R. Baklanov, K.P. Mogilnikov, M. Toney, H.C. Kim, J. Appl. Phys. 94 (2003) 3427.
[2] A. Grill, D.A. Neumayer, J. Appl. Phys. 94 (2003) 6697.
[3] D. Zhao, P. Yang, N. Melosh, J. Feng, B.F. Chmelka, G.D. Stucky, Adv. Mater. (Weinheim, Ger.) 10 (1998) 1380.
[4] S. Baskaran, J. Liu, K. Domansky, N. Kohler, X. Li, C. Coyle, G.E. Fryxell, S. Thevuthasan, R.E. Williford, Adv. Mater. (Weinheim, Ger.) 12 (2000) 291.
[5] C.M. Yang, A.T. Cho, F.M. Pan, T.G. Tsai, K.J. Chao, Adv. Mater. (Weinheim, Ger.) 13 (2001) 1099.
[6] C.M. Whelan, Q.T. Le, F. Cecchet, A. Satta, J.-J. Pireaux, P. Rudolf, K. Maex, Electrochem. Solid-State Lett. 7 (2004) F8.
[7] P. Rouffignac, Z. Li, R.G. Gordon, Electrochem. Solid-State Lett. 7 (2004) G306.
[8] W.J. Ahearn, P.R. Fitzpatrick, J.G. Ekerdt, J. Vac. Sci. Technol. A 3 (2007) 25.
[9] H.J. Lee, E.K. Lin, W.L. Wu, B.M. Fanconi, J.K. Lan, Y.L. Cheng, H.C. Liou, Y.L. Wang, M.S. Feng, C.G. Chao, J. Electrochem. Soc. 148 (2001) F195.
[10] A.M. Hoyas, J. Schuhmacher, C.M. Whelan, M.R. Baklanov, L. Carbonell, J.P. Celis, K. Maex, J. Vac. Sci. Technol. B 23 (2005) 1551.
[11] H.G. Peng, D.Z. Chi, W.D. Wang, J.H. Li, K.Y. Zeng, R.S. Vallery, W.E. Frieze, M.A. Skalsey, D.W. Gidley, A.F. Yee, J. Electrochem. Soc. 154 (2007) G85.
[12] A. Furuya, E. Soda, K. Yoneda, T. Yoshie, H. Okamura, M. Shimada, N. Ohtsuka, S. Ogawa, in: Proceedings of International Interconnect Technology Conference, 7–9 June 2004, 2004, p. 39.
[13] A. Furuya, E. Soda, M. Shimada, S. Ogawa, Jpn. J. Appl. Phys. Part 1 44 (2005) 7430.
[14] L. Parratt, Phys. Rev. 95 (1954) 359.
[15] P.F. Fewster, Rep. Prog. Phys. 59 (1996) 1339.
[16] L.W. Hrubesh, J.F. Poco, Mater. Res. Soc. Proc. 371 (1995) 195.
[17] W.L. Wu, W.E. Wallace, E.K. Lin, G.W. Lynn, C.J. Glinka, E.T. Ryan, H.M. Ho, J. Appl. Phys. 87 (2000) 1193.
[18] W.L. Wu, H.C. Liou, Thin Solid Films 312 (1998) 73.
[19] E. Kondoh, T. Asano, H. Arao, A. Nakashima, M. Komatsu, Jpn. J. Appl. Phys. Part 1 39 (2000) 3919.
[20] M. Yoshimaru, S. Koizumi, K. Shimokawa, J. Ida, in: IEEE Reliability Physics Symposium IEEE, New York, 1997, p. 234.
[21] E.H. Nicollian, J.R. Brews, MOS (Metal Oxide Semiconductor) Physics and Technology, John Wiley & Sons, New York, 1982. p. 532.
[22] V. Jousseaume, M. Fayolle, C. Guedj, P.H. Haumesser, C. Huguet, F. Pierre, R. Pantel, H. Feldis, G. Passemard, J. Electrochem. Soc. 152 (2005) F156.